

Multiple-wavelength Raman lidar measurements of atmospheric water vapor

Sumati Rajan¹, Timothy J. Kane^{1,2} and C. Russell Philbrick^{1,2}

Abstract. Height profiles of atmospheric water vapor obtained using a multiple-wavelength Raman lidar are examined. The water vapor profiles exhibit vertical structure with scales on the order of the resolution of the lidar (75 m). To determine whether such structure is atmospheric in origin, measurements obtained simultaneously in a common volume at two independent wavelengths were compared. Correlation of the gradients of the water vapor profiles obtained from these two wavelengths yielded an average correlation factor of 0.88. It was also observed that for the given meteorological conditions, the vertical structure decorrelated with a time constant of approximately three hours.

Introduction

Water vapor plays a fundamental role in the Earth's weather, climate and other atmospheric processes, hence the need to study its spatial and temporal variability. Currently, routine soundings are made using radiosondes while large scale global variations have been studied via satellite probing employing radiometric techniques. Radiosondes, the common method of measuring atmospheric water vapor, have good spatial resolution but poor temporal resolution which is limited by the interval between balloon launches. Alternatively, radiometers have excellent temporal resolution but poor height resolution. Several types of lidars, however, have been used to monitor the distribution of atmospheric water vapor with excellent spatial and temporal resolution [Grant, 1991]. Extensive work has already been done to calibrate and verify lidar measurements using balloon borne radiosondes [Whiteman et al., 1992]. The total precipitable water vapor measured by both radiometers and lidars has also been compared in order to verify lidar measurements [England et al., 1992]. In this paper we attempt to take this one step further by comparing the measurements from two independent simultaneous lidar measurements.

We have observed that the water vapor profiles measured using a Raman lidar system exhibit fine structure with vertical scales on the order of the altitude resolution of the lidar (in our case 75 m). It is necessary to determine whether these

observations are atmospheric in origin or are an artifact of the measurement. One method to accomplish this would be to compare water vapor measurements obtained simultaneously in a common volume of the atmosphere by two independent lidars [Goldsmith et al. 1994]. Penn State's LAMP (Laser Atmospheric Meamurements Program) lidar system, employing two independent water vapor measuring Raman channels, is the equivalent. In this paper several data sets which display fine vertical structure are presented and analyzed to determine the degree of precision of the Raman technique.

System description

Penn State's LAMP lidar is a monostatic system employing a Nd:YAG laser operating at the doubled (532 nm) and tripled (355 nm) frequencies with a pulse rate of 20 Hz [Philbrick, 1994]. The output power per pulse is approximately 500 mJ at 532 nm and 200 mJ at 355 nm. The backscattered light collected by the f/15 Cassegrain telescope is fed to the detector box via a 1 mm diameter optical fiber (NA= 0.22). The detector system separates the returned signal into the 532 nm and 355 nm Rayleigh channels, and the corresponding Raman nitrogen and water vapor channels (i.e. 607 nm, 387 nm, 660 nm, and 407 nm). The Raman channels have thermally stabilized narrowband filters with bandpasses of 0.3 nm in order to suppress both background noise and the laser line. The backscattered light is detected using cooled PMTs operating in the photon counting mode. Due to the shadowing effects of the secondary mirror of the telescope, as well as the reduction in efficiency due to the telescope/optical fiber system, the lidar system receives a very weak backscattered signal from the first three range bins. Since the statistical noise of the received signal is proportional to the inverse of the square root of the number of photons received, these bins yield very low signal to noise ratios. The following analysis was therefore limited to altitudes ranging from 250 m to 5 km.

It is most convenient to express the lidar water vapor measurement in terms of the water vapor mixing ratio, $w(z)$, which can be expressed as:

$$w(z) = \frac{n_{WV}(z)}{n_{dry\ air}(z)} \frac{M_{WV}}{M_{dry\ air}} = K \frac{S_{WV}(z)}{S_N(z)} \quad (1)$$

where M is molecular weight, n is number density and the subscript WV implies water vapor. Since nitrogen is a constant fraction of dry air, the water vapor mixing ratio can be estimated by taking the ratio of the Raman water vapor backscatter signal (S_{WV}) to the Raman nitrogen backscatter signal (S_N) in any altitude interval. Thus the mixing ratio can be expressed as the second part of equation 1, where the constant of proportionality,

¹Department of Electrical Engineering,

²Applied Research Laboratory,

The Pennsylvania State University, University Park, Pennsylvania

Copyright 1994 by the American Geophysical Union.

Paper number 94GL01993

0094-8534/94/94GL-01993\$03.00

K , is determined from a radiosonde launched concurrently. Taking this ratio eliminates the dependence of the lidar's water vapor measurement on the system characteristics and the atmospheric transmission, since the difference in aerosol scattering at the two wavelengths is minimal. Thus taking this ratio corrects for most of the extinction due to aerosols [Whiteman et al., 1992]. For the sake of brevity, the mixing ratio calculated from the 660nm/607nm ratio will be referred to as the visible water vapor profile and the 407nm/387nm ratio will be called the UV water vapor profile.

Measurements and Discussion

In this paper we will examine data obtained on the nights of August 14 and August 18, 1993 at Pt. Mugu, CA. Both nights were fairly clear with low wind speeds. Although the test period at Pt. Mugu extended from July through October, the 355 nm UV channel was disabled in mid-August, to test different detector sub-systems. Initial tests included lidar-radiosonde comparisons which agreed well with regards to the general shape and characteristics of the two profiles which is consistent with similar comparisons made by Melfi et al [1990]. Often, discrepancies are observed when one attempts to correlate the lidar and radiosonde measurements on finer vertical scales. Such discrepancies can be attributed to the following reasons: 1) the balloon makes almost instantaneous (between 2 and 5 seconds) point measurements at each altitude, while the lidar measurement represents an average value over a given period, 2) the measurements are non-common volume since the balloon drifts, and, 3) measurements are not exactly simultaneous. Hence one can make confident lidar-sonde comparisons only on large scale structures and general trends.

However, on several occasions we have we have noted excellent agreement even on the fine structure observed. (Measurements of atmospheric water vapor fine structure have been reported by other researchers as well [Melfi, et. al. 1991].) An example of one such data set was obtained on August 18, 1993 at Pt. Mugu and is shown in Figure 1. This figure shows

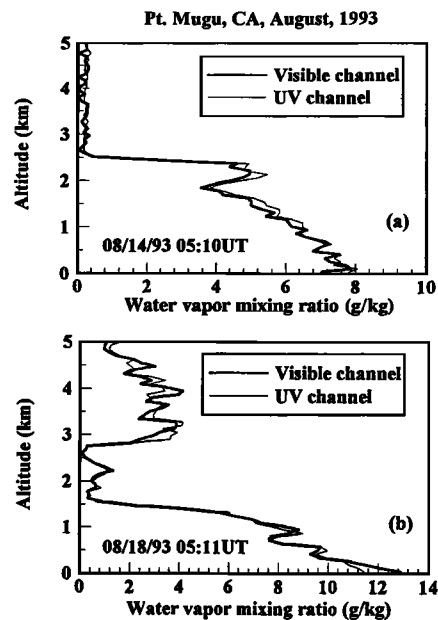


Figure 2. Comparison of water vapor profiles measured by the visible and the UV Raman channels. The data is integrated over 30 minutes with 75 m resolution. Error bars for these curves would be comparable with those in Figure 1.

a typical water vapor profile integrated over thirty minutes, with a vertical resolution of 75 m. The other profile in this figure is the water vapor mixing ratio profile calculated from the radiosonde measurements of relative humidity and temperature obtained from a nearly concurrent Vaisala sonde. On comparing the lidar and radiosonde profiles in Figure 1, we see that the general characteristics of the water vapor profile, i.e. the height of the boundary layer, the profile shape of water vapor between 2500-5000 m, and other features measured by both instruments are consistent.

In Figure 2 we see examples of typical water vapor mixing ratio profiles measured by both the visible and the UV channels starting at 05:10 UT on 8/14/93, and beginning at 05:11 UT on 8/18/93 at Pt. Mugu, CA. These profiles represent half hour integrated data sets with 75 m vertical resolution. Note that these profiles are similar to the 'typical' lidar profile shown in Figure 1, and that the error bars are comparable. Upon visually comparing the two profiles we see that not only is there good agreement in the general profile, but that the fine structure with scales on the order of 200-250m also seems to match well. Except for the laser source the two water vapor channels are independent with regards to detector optics and electronics. Recall that the water vapor mixing ratio is independent of system characteristics such as the laser source power. Hence the counting statistics for each water vapor measurement are independent, which is a key concern for exploring issues related to the precision of lidar measurements. By comparing the visible and the UV water vapor ratios, we are essentially comparing two independent simultaneous common-volume lidar measurements.

To exact a more conclusive result it is necessary to quantify these agreements. Correlating the shapes of the two profiles unfortunately yields correlation coefficients which are biased to the coarser features of the water vapor profiles. One way to eliminate the sensitivity of the correlation to the gross structure

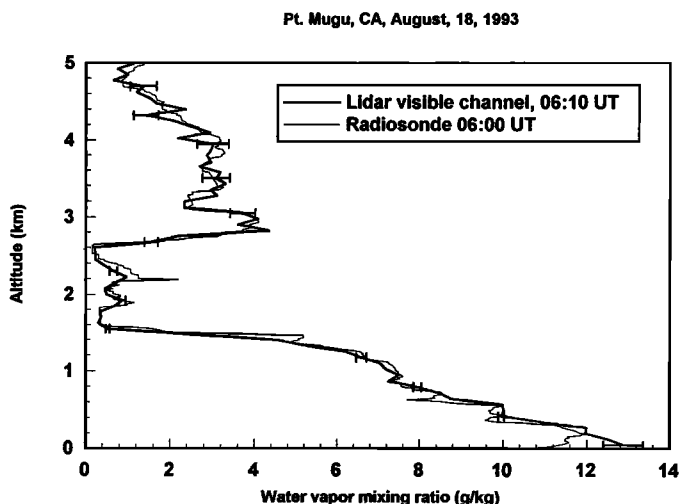


Figure 1. Comparison of water vapor mixing ratio measurements obtained by the LAMP lidar system and a concurrent radiosonde. The one standard deviation error bars based on statistical count are shown on the lidar curve. Radiosonde measurements have approximately 5% accuracy.

of the profile is to subtract an average profile before making comparisons. However, the estimate of an average profile is subjective and prone to errors. We found that an effective method for comparing two lidar profiles is to correlate the vertical gradients. Taking the gradient, g_p , i.e. the change in the water vapor mixing ratio for the change in altitude between two data points (see Equation 2), is equivalent to performing a high pass filter on the data. This suppresses the slowly varying features of the profile, thereby enhancing the sensitivity of the correlation to the finer vertical structure.

$$g_i = \frac{z_{i+1} - z_i}{w(z_{i+1}) - w(z_i)} \quad (2)$$

Figure 3 shows scatter plots relating the gradients of the visible profiles to those of the UV profiles, for the examples shown in Figure 2. Each point on these plots represents the gradient calculated at each height within the altitude range of 250 m to approximately 5 km. The statistical error varies with altitude; however the error for each point is smaller than the block given at each point. The upper limits were 4.6 km for the night of August 14 and 5 km for the night of August 18. Outside this range, the statistical noise was greater and the signal to noise ratio was extremely low. The solid line is the least squares fit to these points. Note that though the spread of points in Figure 3b is noticeably different from the spread seen in Figure 3a, (due to the difference in the shape of the water vapor profile on these two days), the slope of the linear fit of the data points is still on the order of 0.9 for both curves. This slope should be approximately equal to 1. However, since the visible and UV channels are independently calibrated to the radiosonde, slight discrepancies in the calibration may cause one channel's readings to be consistently lower than the other.

Figure 4 shows a similar scatter plot correlating the gradients of the UV and the visible profiles obtained from four 30 minute

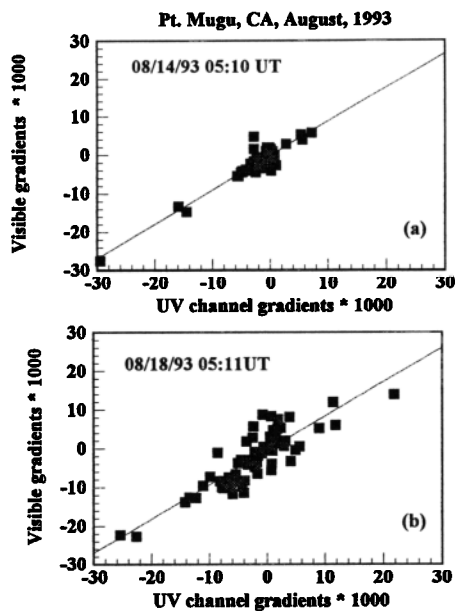


Figure 3. Scatter plots comparing the gradient at each altitude of the water vapor profiles shown in Figure 2. The straight line represents the least squares fit for each plot. The error bars for each point are smaller than the blocks shown.

Pt. Mugu, CA, August 18, 1993, 05:11-07:21 UT

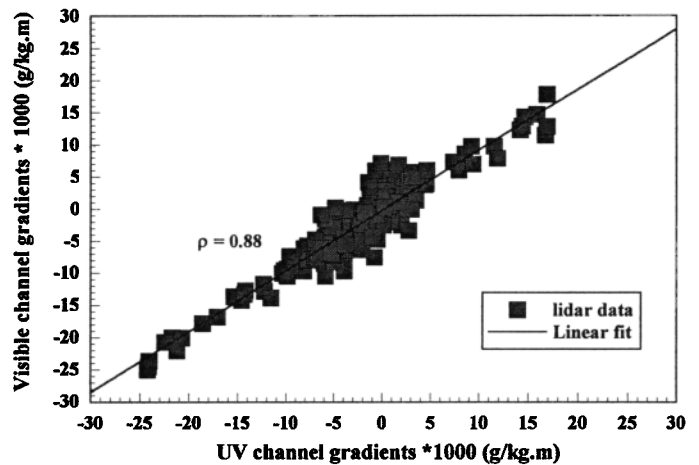


Figure 4. Scatter plot relating gradients of the water vapor profile measured by the visible and the UV channels. The plot represents all data collected on August 18, 1993 between 05:11 and 07:21 UT. The data was integrated over 30 minutes and has 75 m resolution. The error bars on each point are smaller than the blocks shown.

data sets obtained on the night of August 18, 1993. As mentioned above the statistical error varies with altitude but is smaller than the block shown for all points. In both Figures 3 and 4 it is important to note that very few points lie far from the 1:1 ratio line. Those that do are clustered at the origin and can be attributed to statistical spread for very small deviations. The correlation coefficient expected between 2 profiles which are identical except for independent statistical uncertainty of the same magnitude as found in our system was calculated to be 0.97. A least squares fit to the actual data points presented in Figure 4 yields a slope of approximately 1, as expected, with an average correlation coefficient of 0.88 at the highest resolution of the system (75 m) and a data integration time of 30 minutes. This relatively high correlation factor strongly suggests that the fine structure observed is atmospheric in origin.

To further validate the gradient correlation technique, it was applied to several sets of the visible channel's water vapor profiles. Initially a gradient correlation was performed on a profile with itself as a check. This yielded the expected correlation coefficient of 1. Then a gradient correlation was performed on the visible water vapor profile measured at 05:11 UT on August 18, 1993 with the visible water vapor profile measured at 06:10 UT on August 18, 1993, i.e. a 60 minute separation. The average correlation factor obtained here was 0.64. These two profiles are difficult to distinguish by eye or even by standard correlation of the two data sets. However, by using the gradient correlation, they are much easier to distinguish since the decrease in the correlation coefficient (between the simultaneous measurement and measurements made an hour apart) is about 20%. Measurements obtained two hours apart yield a correlation coefficient of 0.54. A similar test, utilizing the gradient correlation method on the first and last data set on August 18, approximately three hours apart, yielded a correlation coefficient of 0.34. This decrease in the correlation coefficient demonstrates the loss of temporal coherence of the

water vapor structure over the entire layer as the time interval increases. For the given weather conditions it appears that the water vapor structure decorrelates with a time constant of about three hours. Hence for this particular case an integration period of 30 minutes was adequate, however further studies should include shorter integration times. Finally, the gradient correlation of two vastly different profiles i.e. the visible water vapor profiles measured on the nights of August 18 and August 14 yielded an expectedly low correlation coefficient of 0.07. The above results are summarized in Table 1.

Conclusions

In several experiments, we have observed that water vapor profiles measured by the UV and visible Raman lidar channels agree well not only in their general shape but also in the "fine structure" observed with scales on the order of the vertical resolution of the system. A gradient correlation technique performed on simultaneous measurements made by the visible and UV channels yielded an average correlation factor of 0.88. Hence, it is evident that this vertical structure is a manifestation of atmospheric phenomena rather than an artifact of the measurement. Using the gradient correlation technique (which is capable of resolving small differences between consecutive data sets) to study the temporal decorrelation of water vapor structure, it was observed that the time constant of the observed

Table 1. Gradient correlation analysis of water vapor profiles with 75m/30min resolution exhibiting temporal decorrelation of water vapor structure.

Profiles compared	Correlation coefficient
Visible channel (self correlation)	1.
Visible channel measurements separated by one hour (8/18/93)	0.64
Visible channel measurements separated by two hours (8/18/93)	0.54
Visible channel measurements separated by three hours (8/18/93)	0.34
Visible channel measurements made on 2 different days (8/14/93 and 8/18/93)	0.07
Simultaneous UV and visible channels (average)	0.88

structure was approximately three hours. This technique may therefore be used to study the temporal evolution of water vapor structure as well as other atmospheric characteristics measured by lidars.

Acknowledgements. The preparation of the LAMP instrument has been supported by the PSU/ARL project initiation funds, PSU College of Engineering, the Navy's Environmental Systems Program Office (SPAWAR PMW-165), Naval Command, Control and Ocean Surveillance Center RDT&E Division and NSF's CEDAR Program. We would also like to thank all the students and staff of the Penn State/ARL lidar lab who have contributed much to the project. These measurements were possible due to the cooperative support of the Geophysics Division of the Naval Air Warfare Center, Point Mugu, CA.

References

- England, M. N., R. A. Ferrare, S. H. Melfi, D. N. Whiteman, and T. A. Clark, Atmospheric water vapor measurements: Comparison of microwave radiometry and lidar, *J. of Geophys. Res.*, **97**, 899-916, 1992.
- Goldsmith, J. E. M., S. E. Bisson, R. A. Ferrare, K. D. Evans, D. N. Whiteman, and S. H. Melfi, Raman lidar profiling of atmospheric water vapor: Simultaneous measurements with two collocated systems, *Bull. of the Amer. Meteor. Soc.*, **75**, 975-982, 1994.
- Grant, W. B., Differential absorption and Raman lidar for water vapor profile measurements: a review, *Opt. Eng.*, **30**, 40-48, 1991.
- Melfi, S. H., D. N. Whiteman, and R. Ferrare, Atmospheric structure revealed by Raman lidar, *Optics & Photonics News*, **2**, 16-18, Oct. 1991.
- Melfi, S. H., D. N. Whiteman, R. Ferrare, and F. Schmidlin, Comparison of lidar and radiosonde measurements of atmospheric moisture profiles, *Tech. Digest, Optical Remote Sensing of the Atmosphere*, Incline Village, NV, 232-234, Feb. 1990.
- Philbrick, C. R., Raman lidar measurements of atmospheric properties, *Proc. of SPIE symposium on atmospheric propagation and remote sensing III*, **2222**, 922-931, 1994.
- Whiteman, D. N., S. H. Melfi and R. A. Ferrare, Raman lidar system for the measurement of water vapor and aerosols in the Earth's atmosphere, *Appl. Opt.*, **31**, 3068-3082, 1992.
- S. Rajan, T. J. Kane, and C. R. Philbrick, Department of Electrical Engineering, The Pennsylvania State University, University Park, PA 16802. (e-mail: sur@ecl.psu.edu, kane@ecl.psu.edu, and crp@ecl.psu.edu)

(Received June 7, 1994; accepted June 30, 1994)